Supporting Information

Real-time Autonomous Control of a Continuous Macroscopic Process as Demonstrated by Plastic Forming

Shun Muroga[a]*, Takashi Honda[b], Yasuaki Miki[a], Hideaki Nakajima[a], Don N. Futaba[a], Kenji Hata[a]

[a]: Nano Carbon Device Research Center, National Institute of Advanced Industrial Science and Technology, Tsukuba Central 5, 1-1-1, Higashi, Tsukuba, Ibaraki, 305-8565, Japan

[b]: Research Association of High-Throughput Design and Development for Advanced Functional Materials (ADMAT), Tsukuba, Ibaraki, 305-8568, Japan

*Corresponding author. E-mail: muroga-sh@aist.go.jp

Experimental Section

Material

A commercially available polycarbonate pellet (Panlite L1225-LL, Teijin Limited) was used for the macroscopic forming process in this study. The rheological properties of this polycarbonate were measured using an oscillatory shear rheometer (AR-2000, TA Instruments, Inc.) as shown in Fig. S1.

Continuous Macroscopic Process

The plastic film forming process was chosen as a typical macroscopic forming process in this study. The pellets were fed into the hopper, melted, and extruded into a T-shaped die, subsequently cooled by air and rollers to form the shape of the film. Our developed process was consisted of following five units: (1) a compounding machine (Labo-plastomill 10C100, Toyo Seiki Co., Ltd.), (2) a co-rotating twin-screw extruder unit (2D15W, Toyo Seiki Co., Ltd.) with a screw diameter of 15 mm, a screw aspect ratio of 17, and two heating blocks, (3) a T-shaped coat-hanger die (MT-60B, Toyo Seiki Co., Ltd) with a slit width of 60 mm, (4) a film haul-off unit (FT2B8, Toyo Seiki Co., Ltd.) with a thermostatic circulating oil bath (NTT-20G, Tokyo Rikakikai Co., Ltd.) to keep the roller temperature constant, and (5) a loss-in-weight feeder (AD-4826A, A&D Company, Limited.) for controlling the feed rate of the pellets to the twin-screw extruder. The appearance of our developed process is shown in Fig. S2.

In-situ Evaluation

A digital single-lens reflex camera (ILCE-6600 & SEL18135, SONY Corporation) and a flat panel light-emitting diode (TH2-83X75SW, CCS, Inc.) were used to observe the appearance of the film. In addition, two linear polarizer sheets (MLPH40L-2, MeCan Imaging, Inc.) and a 1/4 wavelength sheet (MCR140N-2, MeCan Imaging, Inc.) with a retardation of 140 nm were introduced for the crossed Nicols polarization setup with a sensitive tint plate. The main optical axis of the 1/4 wavelength sheet was parallel to the flow direction of the film, while those of the linear polarizer sheets were rotated ±45 degrees from the flow direction. The edges of the film were detected by the image processing based on Hough transform (Fig. S3). A laser displacement meter (CL-P015, Keyence Corporation) was also placed on the roller to measure the film thickness.

Autonomous Real-time Process Control

To achieve autonomous process control, we introduced active learning and decision making based on acquisition function. In essence, active learning guides the autonomous optimization process by prioritizing where to try next, focusing on the most potentially informative conditions. This method is more efficient than traditional methods because it strategically selects the most valuable trials, reducing the number of trials required to optimize the conditions. A Gaussian process regressor based on the Matérn 3/2 kernel function and with a length scale of 1.0 was used to link the relationship between process conditions and target properties. The objective function was set to the negative of the relative mean squared error between the target properties (width, thickness) normalized by their target values. The reason for introducing the sum of squared "relative" errors is to normalize the differences in the number of digits of the properties. For example, the width range is 10 – 40 mm, while the thickness range is 0 - 0.1 mm. The acquisition function for determining the next process conditions was the expected improvement (EI). This approach

focuses on a balance between exploring the uncertain parameter space and exploiting the best parameter predicted by a probabilistic model from previous results. In the context of conducting real-time active learning, it is vital to ensure that the process conditions, particularly the temperature, have reached a steady state. Therefore, a situation where the process temperature falls within the range of the set value ±0.5°C is considered a balanced state. In this state, the average width and thickness of the film are calculated to serve as inputs for the active learning process (Fig. S4). Here, the time-series change of the autonomous control was compared to that of a conventional control that mimics human control which adjusts only single conditions at each step (Fig. S5). Some trajectories of the autonomous controls for different target film dimensions are also shown in Fig. S6.

Computational Environment

A commercial workstation was used to connect all instruments of the system and to run the autonomous control program. The specification of the workstation is Windows 10 for Workstation operating system with a central processing unit of AMD EPYC 7702P (64 cores, 128 threads, 2.0GHz clock speed), a graphics processing unit of NVIDIA GeForce RTX 3090, and 128GB of memory (eight 16GB DDR4-3200 ECC registered memories). The program of autonomous control was performed on a computational environment of python=3.9.7, cuda=11.4.152, with numpy=1.21.5, pandas=1.3.5, scikit-learn=1.0.1, matplotlib=3.5.1, opencv-python=4.5.4.60, and modAL[30].
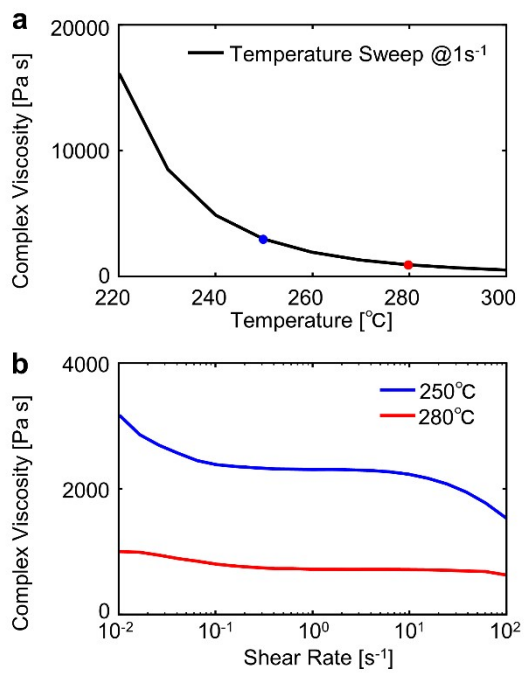
Fig. S1 Rheological properties of the polycarbonate used in this study. (a) Temperature and (b) shear rate dependence on complex viscosity.
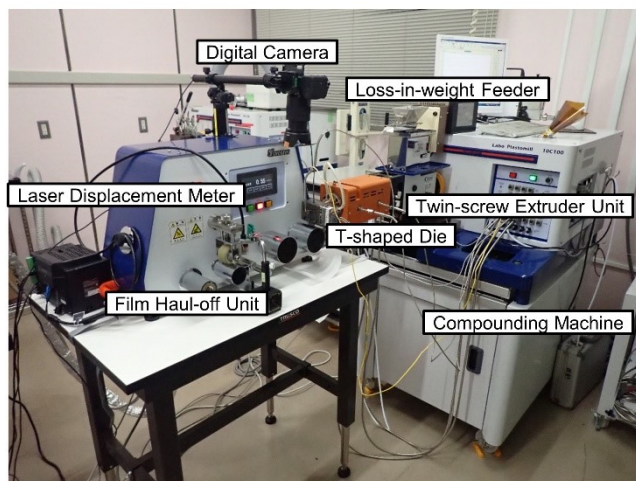
Fig. S2 Appearance of the developed autonomous continuous macroscopic forming process.

a

b
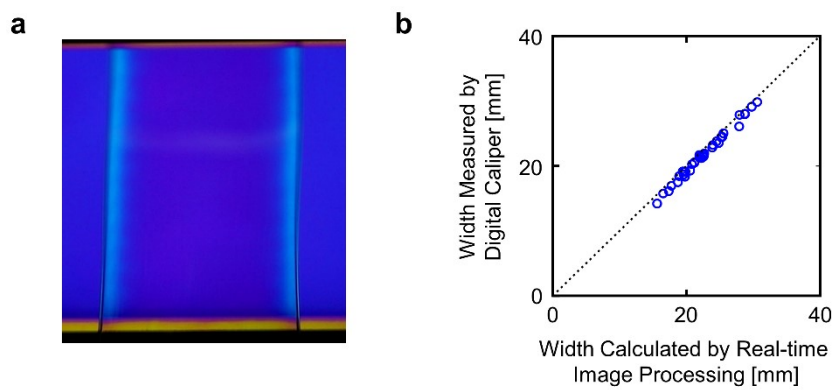
Fig. S3 In-situ evaluation of films using real-time image processing. (a) A typical cross-Nicols polarized image of the film. (b) Comparison of the width calculated by real-time image processing and that measured by digital caliper.
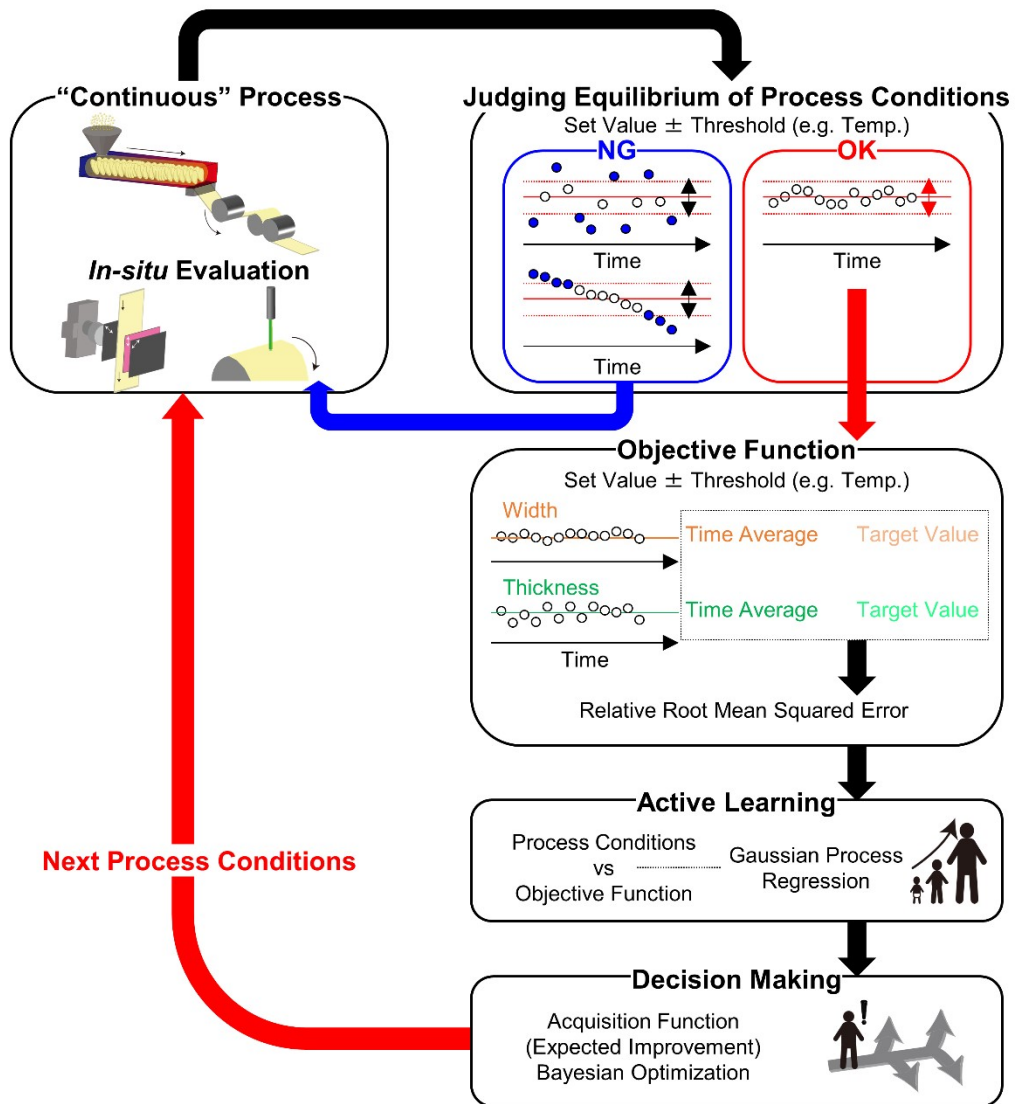
Fig. S4 Workflow of the autonomous control of the continuous process in this study.
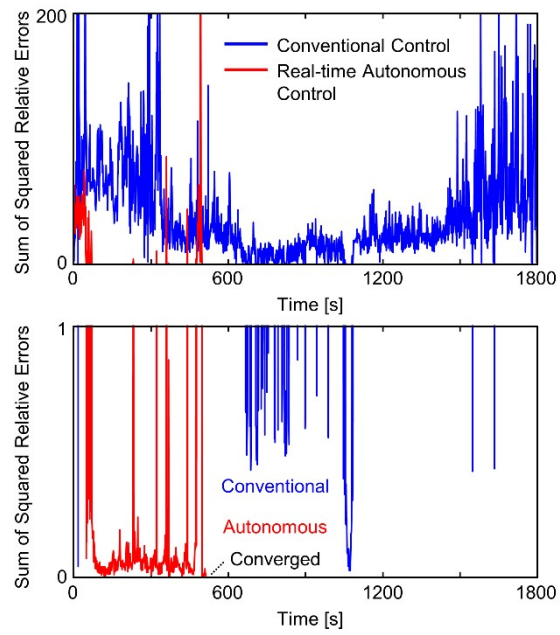
Fig. S5 Comparison of the sum of squared errors of film dimensions between autonomous and conventional control that mimics human operation.
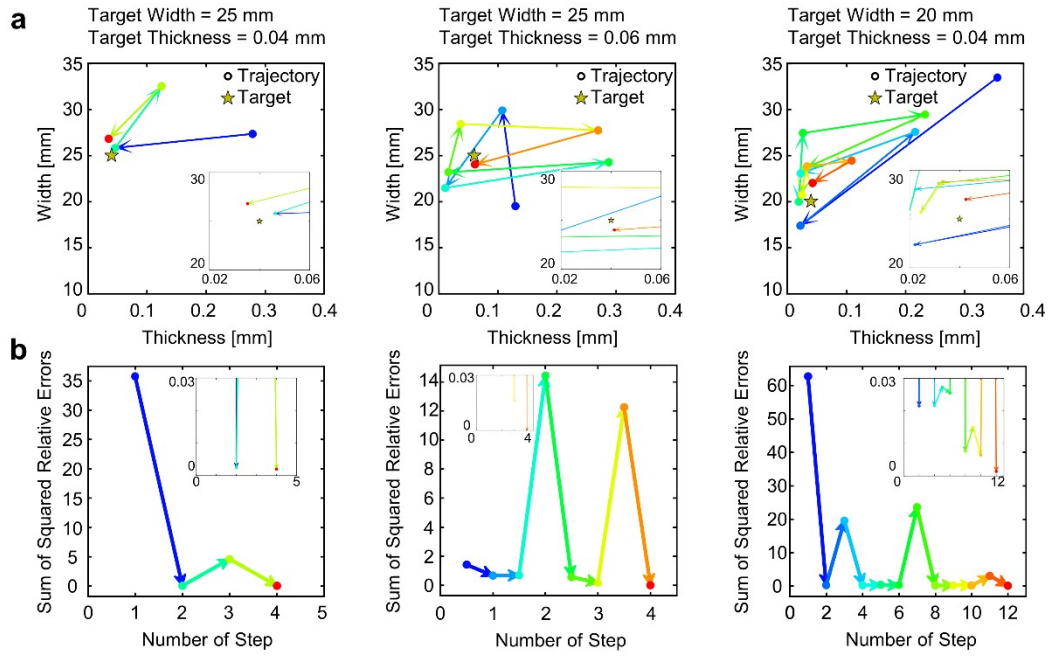
Fig. S6 Autonomous control of different film targets. (a) Trajectory of width and thickness during autonomous control and (b) corresponding sum of squared relative errors for each control step.